

# Hierarchical Human-Motion Prediction and Logic-Geometric Programming for Minimal Interference Human-Robot Tasks

An T. Le<sup>1</sup>, Philipp Kratzer<sup>1</sup>, Simon Hagenmayer<sup>1</sup>, Marc Toussaint<sup>2,3</sup> and Jim Mainprice<sup>1,2</sup>

firstname.lastname@ipvs.uni-stuttgart.de

<sup>1</sup>Machine Learning and Robotics Lab, University of Stuttgart, Germany

<sup>2</sup>Max Planck Institute for Intelligent Systems ; IS-MPI ; Tübingen/Stuttgart, Germany

<sup>3</sup>Technische Universität Berlin ; TUB ; Germany

**Abstract**—In this paper, we tackle the problem of human-robot coordination in sequences of manipulation tasks. Our approach integrates hierarchical human motion prediction with Task and Motion Planning (TAMP). We first devise a hierarchical motion prediction approach by combining Inverse Reinforcement Learning and short-term motion prediction using a Recurrent Neural Network. In a second step, we propose a dynamic version of the TAMP algorithm Logic-Geometric Programming (LGP) [1]. Our version of Dynamic LGP, replans periodically to handle the mismatch between the human motion prediction and the actual human behavior. We assess the efficacy of the approach by training the prediction algorithms and testing the framework on the publicly available MoGaze dataset [2].

## I. INTRODUCTION

As robots become more capable, they will increasingly share space with humans. Consider the case where humans and robots additionally share a task, such as caring for people in a hospital. Robots could tidy, clean, bring lunch to patients, gather medication, or even prepare an operation room. The robot would be collaborating with one or several humans, not only sharing space but also partially executing the task the human is busy with. In such cases the user is interested in having maximal support from the robot while requiring a minimal amount of interference with its own task objectives. Humans do this naturally when they collaborate. For instance, one could put food back into the fridge while the other collects and cleans the dishes. In this paper we propose a framework that can produce such behaviors. We do this by combining hierarchical human motion-prediction and Task and Motion Planning (TAMP) framed as a Logic-Geometric Program (LGP) [1].

For safe and efficient human-robot collaboration it is crucial to account explicitly for the human when generating the robot behavior [3], [4]. Moreover, it is important to predict the human behavior in order to coordinate the human and robot actions, or interact without disturbing the natural flow of the human’s motion. This has been noted in numerous prior works [5], [6]. Hence, human intent and motion prediction is becoming an increasingly important topic of robotics research, which has been recently surveyed by Rudenko et al. [7].

A key challenge for human-motion prediction is to predict movement over a long horizon. This problem arises naturally in the case of sequences of manipulation motions, for ex-

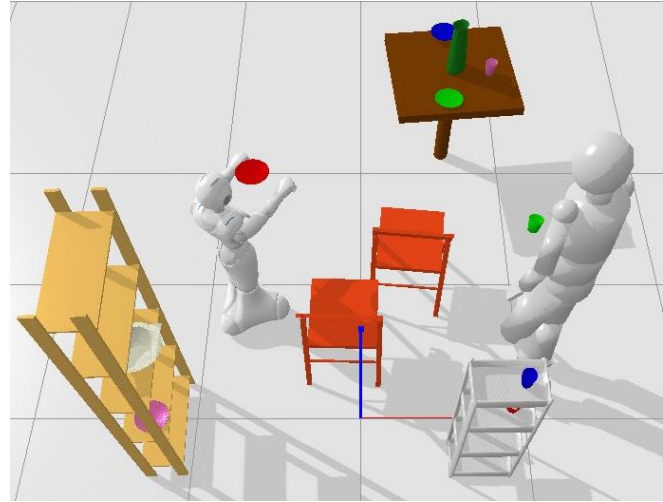


Fig. 1: Pepper carries a plate while the human is carrying a green cup. The motion plan resulting from Dynamic LGP, minimally interferes with the human task while reducing the overall completion time.

ample, when a human and robot have to prepare a table for dinner or tidy a room (see Figure 1). In this work, we propose a hierarchical prediction approach, which can handle such long-term horizon. The general approach is to use two hierarchical levels: symbolic, (i.e. discrete) and geometric (i.e., continuous). For the robot motion planning, we also use these two levels in a TAMP algorithm.

As human motion is the result of complex biomechanical processes that are challenging to model, state-of-the-art work on motion prediction focuses on data-driven models, such as recurrent neural networks [8], [9], [10]. Our prediction approach makes use of Maximum Entropy Inverse Reinforcement Learning [11], to produce a discrete policy, this policy decides what actions to take next based on the symbolic states of the world. At the lowest level we predict movements using a Recurrent Neural Network (RNN), which is trained on the MoGaze dataset [2]. In order to adapt the discrete policy to continuous motion prediction, we introduce goal conditioning to the RNN VRED architecture [8]. We combine two networks, one conditioned on hand target goals for manipulation and another one on pelvis target goals for walking. The high-level policy sequences goals by means of

an intermediate grounding of symbolic layer, resulting in a single trajectory prediction.

Given this prediction, the planning module makes use of LGP to produce minimally interfering plans which support the human with the task objectives. There we devise a symbolic representation of the workspace and the task goal using the Planning Domain Definition Language (PDDL) [12]. Given both the geometric and the symbolic representation, LGP explores the space of skeletons using tree search, which results in a heuristic ranking of symbolic plans. Skeletons are then evaluated with increasing level of accuracy until a feasible plan is found. At the lowest-level a full trajectory is planned using non-linear programming. The optimizer uses an interior point method and a “Gauss-Newton” approximation of the Hessian [13], [14].

We combine human motion prediction and robot motion planning by predicting changes in the symbolic state and planning in the combined symbolic state. We first predict what the human would do and plan for the actions that the human would do last. In order to handle erroneous human motion prediction, we extend the basic formulation of LGP to handle dynamic changes in the workspace.

To summarize the main contributions of the paper:

- We propose a new formulation to produce long-term task sequences for a human-robot team that support the human while minimizing the interference.
- We introduce a new hierarchical motion prediction system which is able to produce full-body prediction in long horizons
- We present results assessing the efficacy of our approach using the MoGaze [2] dataset.

This paper is organized as follows: In Section II we discuss relevant prior work. Section III introduces our framework, and gives information concerning our implementation. In Section V we evaluate our framework on motion capture data. Conclusions are drawn in Section VI.

## II. RELATED WORK

### A. Human-Robot Collaboration

Human-Robot Collaboration (HRC) focuses on robotic systems able to perform joint actions with humans [15], [16]. The robot is a member of a mixed human-robot team, where members share a common goal.

Shared task planning and interactive motion planning allow for higher level collaboration. The notion of *Proxemics* to intelligently account for space-sharing conventions is now well accepted in HRC [17]. To schedule coordinated actions, a lot of work has explored how to model the capabilities of the agents in the workspace [18].

Some works include high-level symbolic planning in order to find a human-aware robot plan [19], [20] and also combining task and motion planning has shown success for human-aware HRC [21], [22].

However, no work proposes to integrate a full hierarchical predictive model of human behavior.

### B. Human-Motion Prediction

Human movement is the result of simultaneous control of hundreds of degrees of freedom. However, muscles are controlled in coordination (i.e., synergies), which yields a low dimensional embedding of motion. Thus, time series techniques such as HMMs, though limited to low dimensional state spaces, have had some success in predicting movement and activities [23].

A lot of work in the area of movement prediction and regression of motion capture data focuses on data driven methods. In these applications less attention is put to reproducing physically correct forces, torques or muscle activation, but rather reproduce plausible movement. Nonlinear function approximators such as Gaussian Processes [24] or Deep Neural Networks [9], [25] have been used to regress large databases of human movement. Recurrent Neural Networks (RNN) are state of the art for predicting short-term high dimensional movements [8], [9], [26].

However, these methods mostly consider very short motions, often less than a second, and therefore are not suitable for predicting long sequences of manipulation tasks. To address this issue, we adapt a RNN architecture and make it goal-conditioned. We use a discrete, high-level policy in order to predict intermediate goals allowing us to predict long motion sequences by chaining the short-term predictions.

### C. Task and Motion Planning

In classical AI, High Level Planning [27] has been studied for decades and many languages and planning paradigms have been developed to solve symbolic planning.

Research in Robotics has sought to integrate such concepts for the purpose of solving motion planning problems involving sequences of tasks such as object manipulation or footsteps. Task and Motion Planning (TAMP) is a sub-field of motion planning and robotics that aims to find multiple intricate and sequential manipulation movements. Usually TAMP involves reasoning on a symbolic level, which provides discrete action sequences, and continuous motion planning, which tries to find motion trajectories fulfilling the discrete action sequence.

Approaches to TAMP often are random sampling methods, [28], [29], [30], constrained-based methods [31], [32] or numerical optimization based methods [1].

In this work we focus on Logic Geometric Programming (LGP) [1], which is an approach combining logic tree search with trajectory optimization techniques, and adapt it to plan a collaborative task in a scenario with a human-robot team. In [33], a human-robot collaboration task is implemented using LGP, where the human prediction is modeled with simple cost terms, and no replanning is performed. To our knowledge, LGP has never been combined with a learned predictive model of human motion.

## III. HIERARCHICAL MOTION PREDICTION & PLANNING

Here we devise the framework for TAMP using a long-term prediction of human motion. We rely on a symbolic decomposition of the task, which we encode using the

Planning Domain Definition Language (PDDL) [12]. We first report on our extension of LGP in Section III-A and then present the motion prediction framework in Section III-B.

### A. Dynamic LGP

For motion planning, we introduce Dynamic LGP, which is a variant of LGP, to solve the minimal interference Human-Robot tasks.

The basic idea of LGP, is to decompose the task with two levels of abstraction. At the highest level we consider a discrete set of actions  $A = \{a_i\}_N^{i=1}$ , for instance move, pick and place (see Figure 4). We call a *skeleton*, a sequence of symbolic actions  $a_{1:K}$ . A fully instantiated plan is then a skeleton, together with a motion trajectory  $x : [0, T] \rightarrow \chi$ , where  $\chi = \mathcal{C} \times \mathcal{H} \times \mathcal{O}$ , the Cartesian product of the robot, human and movable object configuration spaces respectively.

1) *Problem formulation*: An instance  $I$  of Dynamic LGP consists of the following components:

#### Symbolic Domain:

- A set of predicates  $\mathbb{P} = \{P_1(\cdot), \dots, P_N(\cdot)\}$ .
- A set of constants  $\mathcal{O}$  as terms/arguments for predicates  $\mathbb{P}$ .
- A set of all symbolic states  $s \in \mathbb{S}$  in the domain, where each state is a set of grounded propositions from the predicates  $\mathbb{P}$ .
- A set  $A$  of actions  $a = (R, P_+, P_-, E_+, E_-)$  where:
  - $R$  is the set of parameters of the action.
  - $P_+, P_-$  are the sets of positive and negative precondition predicates  $P_+, P_- \subset \mathbb{P}$ .
  - $E_+, E_-$  are the sets of positive and negative effect predicates  $E_+, E_- \subset \mathbb{P}$ .

In our experiments, we adopt a PDDL-syntax to describe the symbolic domain.

**Geometric problem:** Let  $\mathcal{C}$  be the configuration space of the robot and the geometric state at time  $t$ ,  $x_t \in \chi$ . The task is to find a global path  $x : t \mapsto x_t$ , which minimizes the following LGP:

$$\min_{x, a_{1:K}, s_{1:K}} \int_0^{KT} c(x(t), \dot{x}(t), \ddot{x}(t), s_{k(t)}) dt \quad (1a)$$

s.t.

$$x(0) = x_0, \quad h_{\text{goal}}(x(KT)) = 0, \quad g_{\text{goal}}(x(KT)) \leq 0 \quad (1b)$$

$$\forall t \in [0, KT] : h_p(x(t), \dot{x}(t), s_{k(t)}) = 0, \quad (1c)$$

$$g_p(x(t), \dot{x}(t), s_{k(t)}) \leq 0 \quad (1c)$$

$$\forall k \in \{1, \dots, K\} : h_{sw}(x(t), \dot{x}(t), a_k) = 0 \quad (1d)$$

$$s_k \in \text{exec}_{a_k}(s_{k-1}) \quad (1e)$$

$$s_K \in \mathbb{S}_{\text{goal}} \quad (1f)$$

where the path is global continuous  $x$  and contains  $K \in N$  phases, each has fixed duration  $T > 0$ .

In our experiments, the cost function  $c : (q_t, \dot{q}_t, \ddot{q}_t, s) \mapsto c_t \in \mathbb{R}$ , is a combination of differentiable maps, penalizing velocities and accelerations of the robot. Obstacle avoidance and goal manifold are enforced using equality and inequality constraints  $h_p, g_p$  in the phase  $k(t) \in [t/T]$  conditioned on a discrete symbolic state  $s_k \in \mathbb{S}$ .

To impose transition conditions between phases, the switch functions  $h_{sw}, g_{sw}$  define equalities and inequalities constraints conditioned on the transition action  $a_k$ . We assume that the equality and inequality functions are differentiable.

2) *Solving LGP*: To search the symbolic domain for a skeleton satisfying all constraints, the action set  $A$  has to be grounded with the constants set  $\mathcal{O}$  [34], resulting in the grounded action set  $A_g$ .

The most basic operations for searching are the feasibility check and the state transition. In this case, the operations can be formally stated as:

- **Action feasibility check**: A grounded action  $a = (R, p_+, p_-, e_+, e_-) \in A_g$ , in which  $p_+, p_-, e_+, e_-$  are the positive and negative grounded propositions of the preconditions and the effects, is applicable to  $s$  iff  $p_+^a \subset s$  and  $p_-^a \cap s = \emptyset$  with  $\forall s \in \mathbb{S}$ .
- **State transition**: new state  $s' = \text{exec}_a(s) = (s \setminus e_-) \cup e_+$  with  $\forall s, s' \in \mathbb{S}$ .

For a given symbolic goal set  $\mathbb{S}_{\text{goal}} \subset \mathbb{S}$ , these two operations, allow us to instantiate a search process using any tree search algorithm (i.e., depth first, breadth first, etc).

If a skeleton feasible skeleton  $a_{t:K}$  leading to symbolic goal state  $s^g \in \mathbb{S}_{\text{goal}}$  is found, a Non-Linear “trajectory optimization” Program (NLP) is defined. The NLP considers geometric switches in the system kinematics with long-term dependencies. In our implementation we use an interior point method [13], [14] to optimize this NLP.

3) *Single planning*: Given the dynamic LGP instance  $I$  and current symbolic state  $s_0$ , we define the set of all skeletons leading to  $\mathbb{S}_{\text{goal}}$  as:

$$\Gamma(s_0, \mathbb{S}_{\text{goal}}, I) = \{a_{1:K} : \forall_{i=1}^K a_i \in A_g, s_i = \text{exec}_{a_i}(s_{i-1}), s_K \in \mathbb{S}_{\text{goal}}\} \quad (2)$$

For search efficiency, we define a simple heuristic to guide the search as the symbolic distance from the current state and the goal. The distance is defined as:

$$h(s) = n(s_+^g \setminus s) + n(s_-^g \cup s) \quad (3)$$

where  $n(s)$  is the cardinality of the state, i.e. the number of grounded propositions.  $s_+^g, s_-^g$  are the positive and negative proposition set of the goal state  $s^g \in \mathbb{S}_{\text{goal}}$ .

Using the heuristic, we search through the symbolic domain for all tie shortest solutions using Dijkstra algorithm.

Once all tie skeletons are found, we rank them by grounding them using simple interpolation paths and computing their costs defined in Equation (1a). We then solve the NLP instance in increasing cost order until a feasible solution is found.

To achieve human avoidance in single planning at the geometric level, we populate the human positions as obstacles along the human prediction trajectory. This ensures the worst-case scenario, in which the robot finds a collision-free trajectory at the beginning with single planning.

---

**Algorithm 1:** Dynamic LGP

---

**input:** Init state  $x_0$ , goal set  $\mathbb{S}_{\text{goal}}$   
 Infer symbolic state  $s_0$  from  $x_0$ ;  
 Search  $\Gamma_0(s_0, \mathbb{S}_{\text{goal}}, I)$ ;  
 Set  $\kappa = a_{1:K_0} \in \Gamma_0$  as best feasible skeleton;  
 Set elapsed time  $\tau = 0$ ;  
**while**  $\mathbb{S}_{\text{goal}}$  not reached at current  $t$  **do**  
     Update system kinematics and human position;  
     Infer current symbolic state  $s_t$ ;  
     **if**  $\mathbf{F}(\kappa, s_t) = 0$  **then**  
         Search  $\Gamma_t(s_t, \mathbb{S}_{\text{goal}}, I)$ ;  
         Update  $\kappa = a_{1:K_t} \in \Gamma_t$  as best feasible skeleton;  
         Set elapsed time  $\tau = 0$ ;  
     **end**  
     Optimize NLP (Level 3 in [1]) of  $\kappa$  from time  $\tau$ ;  
     Execute current action of the skeleton  $\kappa$ ;  
      $\tau = \tau + 1$ ;  
     Wait for next trigger;  
**end**

---

(on X Y)	check if exists a stable 3D $xy\phi$ joint from X to Y
(at X Y)	check if $\ x_X - x_Y\ _2 \leq r  r \in \mathbb{R}$
(carry X Y)	check if exists a stable free joint (6D) from X to Y

TABLE I: Predicate inference

4) *Dynamic planning.* As the actual human behavior may deviate from the prediction, the motion trajectory or the skeleton  $a_{1:K}$  may become sub-optimal or even unfeasible.

Hence a crucial component for dynamic LGP is to infer the current symbolic state from the current environmental condition. For example, the predicate (on X Y) is inferred by checking in the system kinematic tree if there is a stable 3D  $xy\phi$  joint from X to Y. Table I describes our setup symbolic inference for the predicates using the system kinematics. Specifically, querying (human-carry, ?x - object) or (agent-carry, ?x - object) predicates can be done using (carry X Y) check. This is the mechanism to encode the human intention to the planner symbolically.

In dynamic planning, the executing skeleton at the current time  $t$  needs to be checked for feasibility, both symbolically and geometrically. Formally, given the current inferred symbolic state  $s_t$ , the skeleton feasibility at the current time  $t$  is defined as:

$$\mathbf{F}(a_{1:K}, s_t) = \begin{cases} 1 & s_0 = s_t, \exists x : [t, KT] \rightarrow \mathcal{C} : (1b) - (1f) \\ 0 & \text{otherwise} \end{cases} \quad (4)$$

Algorithm 1 describes the main execution of our dynamic LGP formulation. The main idea is to enable the replanning capability for both: symbolic and geometric levels of LGP, given the current symbolic and geometric state  $x_t$ ,  $s_t$ .

Initially, similar to single planning in Section III-A.3, the algorithm finds the best feasible skeleton at the beginning and sets it to be the current executing skeleton  $p \in \Gamma$ . For each

Start State	(0, 4, 0, 1, 0, 3, 1, 0, 1, 2)
Actions	Go to white shelf Pick up cup Go to table Place
End State	(1, 3, 0, 1, 0, 3, 1, 0, 1, 0)

TABLE II: Example high-level trajectory

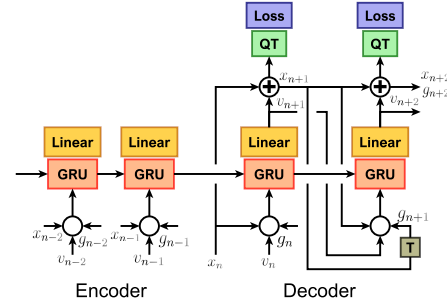


Fig. 2: Structure of the VRED [8] with the goal input added.

replanning trigger, the algorithm checks for actual symbolic and geometric feasibility  $\mathbf{F}(p, s_t)$  of the current executing skeleton.

If the skeleton  $\kappa$  is feasible, the NLP is optimized for  $\kappa$  from the elapsed time  $\tau$ , i.e.,  $\forall t \in [\tau, KT]$ , given the current system kinematics condition. Otherwise, it discards the current executing skeleton and resets the elapsed time  $\tau = 0$ . The single planning is triggered to replan a new skeleton solution set  $\Gamma_t(s_t, \mathbb{S}_{\text{goal}}, I)$  and optimize for the current best feasible skeleton. One may notice the elapsed time  $\tau$  for the current executing skeleton is an implementation detail; however, it plays a crucial role in keeping track remaining execution time for the fixed duration phases of LGP.

### B. Long-Term Motion Prediction using Hierarchies

The motion prediction layer infers likely symbolic and geometric changes in the workspace, given an initial symbolic state  $s_t$  and a geometric state  $x_t$ . Recall that the geometric state  $x_t = (q_t, h_t, o_t)$ , concatenates  $q_t$  is the robot,  $h_t$  the human, and  $o_t$  the movable object configurations. The feasibility of a skeleton  $\kappa$  can then be checked with  $\mathbf{F}(\kappa, s_t)$  defined in Equation 4.

At the top-level, our hierarchical motion prediction uses Maximum Entropy Inverse Reinforcement Learning (MaxEnt IRL) [11] and a low-level which performs full-body motion prediction conditioned on sub-goals given by the top-level.

1) *Goal-Conditioning:* To be able to use motion prediction as a sub-policy, we do not only need a sequence-to-sequence mapping but also need it to be goal-conditioned.

Thus, we need a predictive function  $h_{t+1:T} = f(h_{0:t}, g^*)$  that computes a trajectory of future human states  $h_{t+1:T}$  given previous observed states  $h_{0:t}$  and a goal  $g^*$ . We use VRED, a recurrent neural network-based model for predicting motion [8] and make it goal-conditioned by adding a three-dimensional position  $g_t$  to the input of the network at every timestep (see Figure 2). The goal input  $g_t$  is relative

to the coordinate frame of the human and thus changes every timestep.

Particularly, we train two networks, one conditioned on hand target goals for manipulation and another one on pelvis target goals for walking. The network is trained on full-body, kinematic motion trajectories. We use a mean squared distance loss between the base position and a quaternion loss between joint angles. We add an additional loss  $l_{\text{goal}} = |g_T - \phi(x_T)|^2$  penalizing the distance between the input goal position and the predicted goal position at the last timestep  $T$  of the prediction, using a forward kinematic layer  $\phi$ .

After training, different trajectories can be generated by varying the goal input manually. Composing multiple sub-goals can be used for sequential long-term motion predictions of the human.

2) *Network State Representation*: We learn a policy  $\pi$  that can solve a high-level task. Therefore, we simplify the state-space to a symbolic representation and use tabular MaxEnt IRL to retrieve our policy.

MaxEnt IRL is based on state frequency calculations. For the MoGaze dataset (see Subsection IV), the discretized state is given by the number of objects on a location and the human position as follows: (cups-table, cups-shelf1, cups-shelf2, plates-table, plates-shelf1, jugbowl-table, jugbowl-shelf1, jugbowl-shelf2, humanPos). The action space is discretized similarly. An example skeleton can be seen in Table II.

We use heuristics for interfering the exact goal for the human hand or pelvis, for example, by computing the closest point on the table to the human which is not occupied. The heuristics could be further improved by the use of human intention prediction as in [35].

The full long-term prediction is achieved by obtaining the skeleton from the high level policy  $\pi$ , extracting the goals for the low-level from the heuristics according to the actions in the trajectory, and using the goal-conditioned RNN to obtain a sequence of full-body trajectories corresponding to the high-level actions.

#### IV. DATASET

We test our framework on the MoGaze dataset [2]. The dataset contains 180 minutes of long, full-body motion sequences for six humans, with 1627 pick and place actions being performed.

Besides human data, the dataset contains object data for two shelves, a table, and 10 movable objects like cups and plates. The participants performed simple manipulation tasks, such as setting up the table for a fixed number of persons or putting a set of specified objects onto one of the shelves. This makes the dataset well suited for our application.

#### V. EXPERIMENTS

Here we report three types of experiments. First, we report results on hierarchical motion prediction. Then we report two sets of experiment using LGP, for coordinated human-robot tasks. In the first, we report a large scale experiment on 63 segments of setting up the table for 2-3 persons, where we

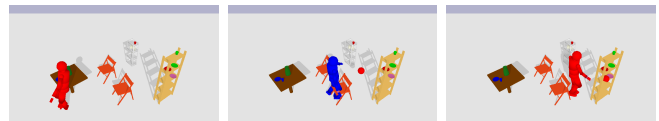


Fig. 3: Examples of predictions when mapping the learned policy of the IRL algorithm to our goal conditioned VRED networks.

```
(define (domain set_table)
  (:requirements :typing)
  (:types location object)
  (:constants
    table small_shelf big_shelf - location
    cup_red cup_green cup_blue cup_pink plate_red plate_green
    plate_blue jug bowl - object
  )
  (:predicates
    (agent-at ?l - location)
    (on ?x - object ?l - location)
    (agent-free)
    (agent-avoid-human)
    (agent-carry ?x - object)
    (human-carry ?x - object)
  )
  (:action move
    :parameters (?l - location)
    :precondition ()
    :effect (and (not (agent-at ?*)) (agent-at ?l)))
  )
  (:action pick
    :parameters (?x - object ?l - location)
    :precondition (and (agent-at ?l) (on ?x ?l) (not (human-carry ?x))) (at
      start (agent-free)))
    :effect (and (not (on ?x ?l)) (not (agent-free)) (agent-carry ?x)))
  )
  (:action place
    :parameters (?x - object ?l - location)
    :precondition (and (agent-at ?l) (agent-carry ?x))
    :effect (and (not (agent-carry ?x)) (on ?x ?l) (agent-free)))
  )
)
```

Fig. 4: PDDL-syntax symbolic domain of set-table task.

use a degraded ground-truth trajectory as the prediction. In the second, we report results on the full pipeline using only 8 segments.

#### A. Long-Term Motion Prediction using Hierarchies

We first compare the original VRED implementation with the VRED conditioned on goal inputs on the MoGaze dataset. Results show that the goal-conditioned prediction network achieves both a better angular loss of 7.99 instead of 10.14 and a significantly better position loss of 3.84 instead of 12.56, than the network without goal-conditioning. This is expected because the goal-conditioned network uses oracle information of the goal position.

To test the accuracy of the high-level policy, we extracted the task of setting up the table for one person from the dataset. We then run tabular MaxEnt IRL, showed that the learned policy solved the task in 80% of the cases. However, a perfect imitation was achieved solely in 16% of the test runs of the cross-validation. This is because the algorithm is limited by our symbolic state and action representation. Including more complex state features, e.g., from the 3d environment, could further improve the algorithm.

In Figure 3 we combine the learned policy from the MaxEnt IRL algorithm with our goal-conditioned neural networks for walking and manipulating objects and report three example frames. As one can see the human is predicted to attempt a grasping action (left), a walking action (middle), and a placing action (right), respectively. Note that for the

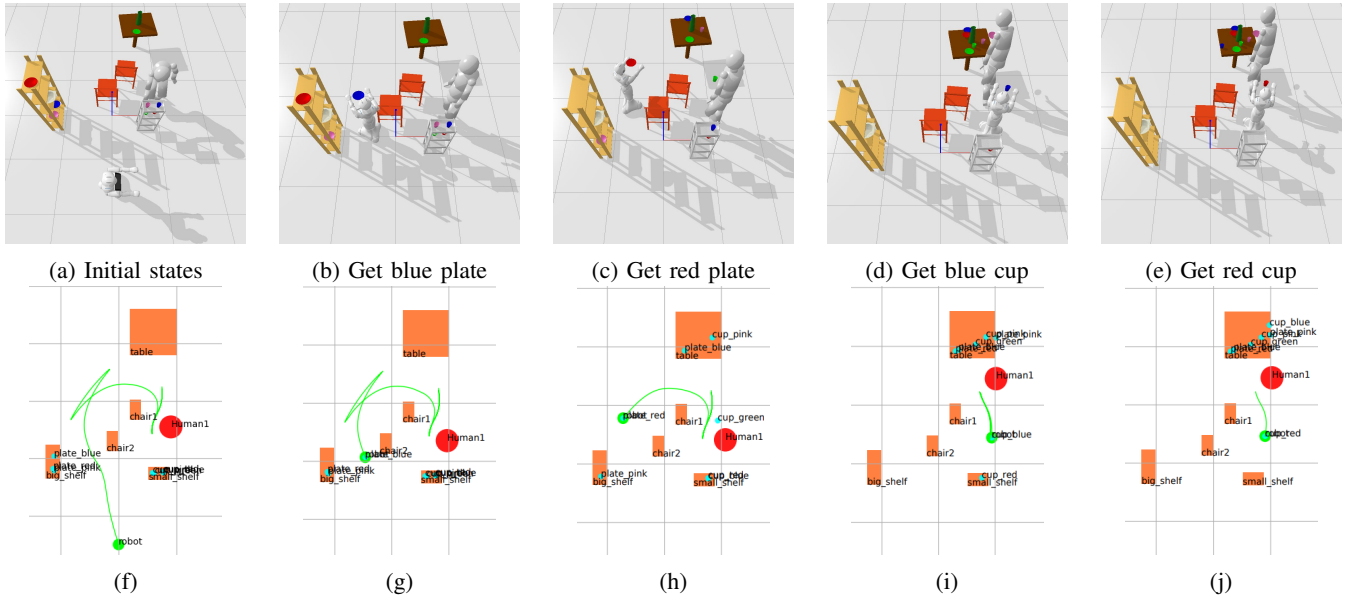


Fig. 5: Dynamic LGP demonstration. Note that in the bottom row images, the robot trajectory is green.

walking action the human collides with a chair, as the model is not aware of scene geometry. In future work this could be avoided by using a prediction method that accounts for the scene, such as [26].

### B. Dynamic LGP with Human Ground Truth

To test Dynamic LGP, we design the PDDL-syntax domain following the available objects in the MoGaze dataset. Figure 4 presents the domain for a set-table task, which consists of a set of necessary predicates and a set of actions, in which the robot and the human cooperate to pick and place objects setting the dinner table for 2-3 persons.

We select 63 dataset segments for this task, and automate inferring the start symbolic state from the environment kinematics. We define the robot goal for each segment, e.g.  $s_0 = \{(agent-free), (agent-avoid-human), (on cup-green big-shelf), (on plate-blue small-shelf)\}$  and the goal state  $s_g = \{(on cup-green table), (on plate-blue table)\}$ .

In this experiment we directly feed the human trajectory ground truth into the Dynamic LGP. We randomly remove a part of the human trajectory in the dataset for each segment to simulate human prediction data.

The overall task Intersection over Union (IoU) between the set of objects the human and the robot must place on the table is  $0.64 \pm 0.30$ . In other words, most of the robot task instance has more than half of the objects to pick and place overlapping with the human task. Dynamic LGP needs to recognize the overlapping part and plan accordingly.

The replanning trigger rate is set every 10 timesteps. The *move* action has fixed duration of 30 timesteps, the *pick* and *place* actions both have fixed duration of 5 timesteps. The sampling rate is 10Hz.

We pause the simulation environment each time the planner is triggered so that the robot reacts in time to avoid the human obstacle. An example of a dynamic LGP run is

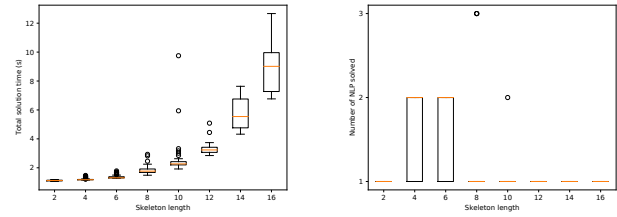


Fig. 6: Total time (left) and number of solved NLPs (right) to find an overall feasible solution over skeleton length.

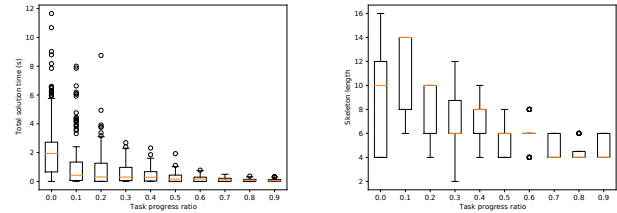


Fig. 7: Total time (left) to find an overall feasible solution and skeleton length (right) over task progress.

demonstrated in Figure 5, where the task instance consists of 7 objects to pick and place. The robot executes pick and place for 4 objects, and the human executes the other 3 objects.

We then run two planning modes; single planning and dynamic planning for each of the 63 segment. The task instance is considered successful if, at the end of the robot trajectory, the inferred symbolic state is in the goal set  $\mathbb{S}_{goal}$ . For dynamic planning, the task fails when the timeout for Algorithm 1 is reached while the goal set is not satisfied. For single planning, the task fails when no feasible skeleton is found.

Table III summarizes the statistics in terms of success rate, symbolic planning time, task time reduction (i.e., the original time taken by the human to perform the task in the dataset

	Single planning	Dynamic planning
Success rate	84.1%	95.2%
Symbolic plan time	$0.032 \pm 0.036(\text{sec})$	$0.045 \pm 0.053(\text{sec})$
Task time reduction	$0.577 \pm 0.107$	$0.683 \pm 0.099$
Path ratio	1.000	$0.584 \pm 0.148$
LGP replan count	-	$4.83 \pm 2.21$

TABLE III: Dynamic LGP with Human Ground Truth

	Single planning	Dynamic planning
Success rate	91.2%	100%
Symbolic plan time	$0.0005 \pm 0.0001(\text{sec})$	$0.0006 \pm 0.0002(\text{sec})$
Task time reduction	$0.298 \pm 0.078$	$0.300 \pm 0.100$
Path ratio	1.000	$0.626 \pm 0.155$
LGP replan count	-	$3.0 \pm 0.87$

TABLE IV: Dynamic LGP with Human Prediction

compared to the execution time with support from the robot) and path ratio (i.e., the ratio of distance traveled by the robot, with the distance of single planning is the baseline). Each category is reported in mean and standard deviation over all task instances. All experiments have been performed with an AMD Ryzen 7 5800X @ 3.8GHz.

As one can see the single planning success rates are lower than dynamic planning. This is expected since the single planning does not account for potential mismatch between the degraded ground truth and the actual ground truth.

Figure 8 depicts the recorded trajectories of both planning modes and the human trajectory in a task instance. We see that the dynamic mode plans a much shorter trajectory going between the shelf and the table because the only human obstacle constraint is efficiently updated at every trigger. We also see in Table III that the trajectory length of single planning is almost twice of dynamic planning (i.e., path ratio).

Surprisingly, the experiment shows that the executing symbolic skeleton in dynamic planning is usually invalid over task progress. Hence full LGP replanning is triggered frequently. This shows that the replanning capability is crucial in a dynamic environment, such as working with humans, since the symbolic state inferred from the environment is rapidly changed.

Figure 6 reports both the total solution time and the number of NLPs that have to be solved to find a feasible solution. As can be seen, most of the time only one NLP is needed to reach a feasible solution. This implies that usually for this task, the lowest cost skeleton is feasible. In other cases, more NLPs need to be solved due to the dynamic characteristic of the task.

Generally, the longer the action skeleton, the longer it takes to solve one NLP. The figure shows a median runtime of about 9 sec for the longest sequence length of 16, with  $\approx 450$  time steps to optimize in an NLP. This time step correspond the time discretization of interior point trajectory optimization algorithm [13], [14]. Notice in Figure 7 that in some cases, the action skeleton length increases as the task progresses. The skeleton length’s median is 6 at task progress ratio 0.3, then increases to 8 at task progress ratio 0.4. This implies that the LGP replan sometimes has to resort to longer

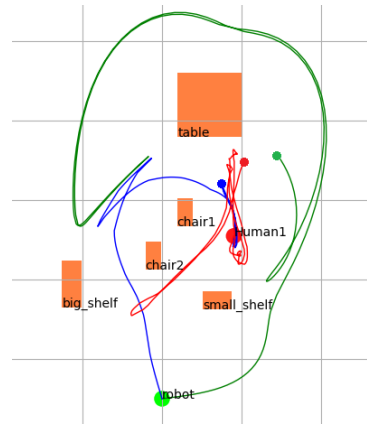


Fig. 8: Recorded actual trajectories of single planning (green), dynamic planning (blue) and actual human trajectory (red) on the workspace.

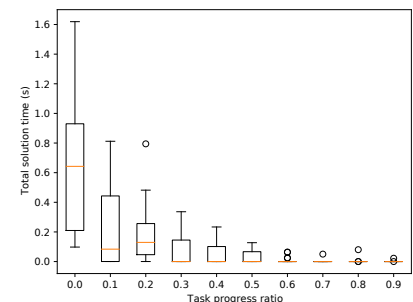


Fig. 9: Total time to find an overall feasible solution over task progress with human prediction.

action skeletons with higher costs as shorter skeletons are infeasible.

### C. Dynamic LGP with Long-Term Prediction

In this experiment, we choose 8 data segments from MoGaze, and produce the Long-Term Prediction outputs as described in Section III-B.

For each segment, we run 5 task instances to capture the human motion prediction statistics due to its stochasticity. The settings are the same as in Section V-B. The overall task IoU between the robot and the human objects is  $0.34 \pm 0.13$ . Obviously, this IoU is less than Human Ground Truth experiment since in the Human Ground Truth experiment the human trajectory is used directly.

Table IV reports task statistics for this experiment. Statistics agree with Table III, which shows that dynamic planning has higher success rates and produces shorter paths and needs slightly more time to complete than single planning.

Figure 9 also shows decreasing total solution times as the task progresses with human prediction. Note that the planning time are an order of magnitude lower, as the task includes less objects.

## VI. CONCLUSIONS & FUTURE WORK

Our experiments show that Dynamic LGP is able to produce plans that have higher success rate than single

planning. These plans also reduce the total time to execute the task by a factor approaching 2, which is what one would expect when two agents collaborate at a task.

In future work, we aim to include collision avoidance in our hierarchical motion prediction framework and produce fullbody robot motions using a Level 2 NLP for LGP (we refer the reader to [1]) to handle complete robot grasping configurations. We also plan to port these results to the Pepper robot of the University of Stuttgart.

## ACKNOWLEDGMENT

This work is partially funded by the research alliance “System Mensch”. The authors thank the International Max Planck Research School for Intelligent Systems (IMPRS-IS) for supporting Philipp Kratzer.

## REFERENCES

- [1] M. Toussaint, “Logic-geometric programming: An optimization-based approach to combined task and motion planning,” in *IJCAI*, 2015, pp. 1930–1936.
- [2] P. Kratzer, S. Bihlmaier, N. B. Midlagajni, R. Prakash, M. Toussaint, and J. Mainprice, “Mogaze: A dataset of full-body motions that includes workspace geometry and eye-gaze,” *IEEE Robotics and Automation Letters*, vol. 6, no. 2, pp. 367–373, 2020.
- [3] A. Bauer, D. Wollherr, and M. Buss, “Human–robot collaboration: a survey,” *International Journal of Humanoid Robotics*, vol. 5, no. 01, pp. 47–66, 2008.
- [4] T. Kruse, A. K. Pandey, R. Alami, and A. Kirsch, “Human-aware robot navigation: A survey,” *Robotics and Autonomous Systems*, vol. 61, no. 12, pp. 1726–1743, 2013.
- [5] B. D. Ziebart, N. Ratliff, G. Gallagher, C. Mertz, K. Peterson, J. A. Bagnell, M. Hebert, A. K. Dey, and S. Srinivasa, “Planning-based prediction for pedestrians,” in *2009 IEEE/RSJ International Conference on Intelligent Robots and Systems*. IEEE, 2009, pp. 3931–3936.
- [6] J. Mainprice and D. Berenson, “Human–robot collaborative manipulation planning using early prediction of human motion,” in *IEEE/RSJ Int. Conf. on Intel. Robots And Systems (IROS)*, 2013.
- [7] A. Rudenko, L. Palmieri, M. Herman, K. M. Kitani, D. M. Gavrila, and K. O. Arras, “Human motion trajectory prediction: A survey,” *The Int. Journal of Robotics Research*, p. 0278364920917446, 2019.
- [8] H. Wang and J. Feng, “Vred: A position-velocity recurrent encoder-decoder for human motion prediction,” *arXiv preprint arXiv:1906.06514*, 2019.
- [9] J. Martinez, M. J. Black, and J. Romero, “On human motion prediction using recurrent neural networks,” in *IEEE Conf. on Computer Vision and Pattern Recognition (CVPR)*. IEEE, 2017.
- [10] D. Pavillo, C. Feichtenhofer, M. Auli, and D. Grangier, “Modeling human motion with quaternion-based neural networks,” *Int. Journal of Computer Vision*, pp. 1–18, 2019.
- [11] B. D. Ziebart, A. L. Maas, J. A. Bagnell, and A. K. Dey, “Maximum entropy inverse reinforcement learning,” in *Aaai*, vol. 8, 2008, pp. 1433–1438.
- [12] D. McDermott, M. Ghallab, A. Howe, C. Knoblock, A. Ram, M. Veloso, D. Weld, and D. Wilkins, “Pddl—the planning domain definition language,” 1998.
- [13] J. Mainprice, N. Ratliff, M. Toussaint, and S. Schaal, “An interior point method solving motion planning problems with narrow passages,” in *IEEE Int. Symp. on Robot and Human Interactive Communication (RO-MAN)*, 2020.
- [14] J. Mainprice, “bewego: Differentiable kinetics optimization library,” 2019–2021. [Online]. Available: <https://github.com/humans-to-robots-motion/bewego>
- [15] A. M. Bauer, D. Wollherr, and M. Buss, “Human–Robot Collaboration - a Survey,” *I. J. Humanoid Robotics*, vol. 05, no. 01, pp. 47–66, 2008. [Online]. Available: <https://www.worldscientific.com/doi/abs/10.1142/S0219843608001303>
- [16] A. Ajoudani, A. M. Zanchettin, S. Ivaldi, A. Albu-Schäffer, K. Kosuge, and O. Khatib, “Progress and prospects of the human–robot collaboration,” *Autonomous Robots*, vol. 42, no. 5, pp. 957–975, Nov. 2017. [Online]. Available: <http://dx.doi.org/10.1007/s10514-017-9677-2>
- [17] T. Kruse, A. K. Pandey, R. Alami, and A. Kirsch, “Human-aware robot navigation: A survey,” *Robotics and Autonomous Systems*, vol. 61, no. 12, pp. 1726–1743, Dec. 2013. [Online]. Available: <http://dx.doi.org/10.1016/j.robot.2013.05.007>
- [18] G. Hoffman and C. Breazeal, “Cost-based anticipatory action selection for human–robot fluency,” vol. 23, no. 5, pp. 952–961, 2007.
- [19] R. Alami, A. Clodic, V. Montreuil, E. A. Sisbot, and R. Chatila, “Task planning for human–robot interaction,” in *Proceedings of the 2005 joint conference on Smart objects and ambient intelligence: innovative context-aware services: usages and technologies*, 2005, pp. 81–85.
- [20] S. Lemaignan, M. Warnier, E. A. Sisbot, A. Clodic, and R. Alami, “Artificial cognition for social human–robot interaction: An implementation,” *Artificial Intelligence*, vol. 247, pp. 45–69, 2017.
- [21] M. Gharbi, R. Lallement, and R. Alami, “Combining symbolic and geometric planning to synthesize human-aware plans - toward more efficient combined search,” *IROS*, pp. 6360–6365, 2015. [Online]. Available: <http://ieeexplore.ieee.org/document/7354286/>
- [22] B. Busch, M. Toussaint, and M. L. 0001, “Planning Ergonomic Sequences of Actions in Human–Robot Interaction,” *ICRA*, 2018. [Online]. Available: <https://dblp.org/rec/conf/icra/BuschT018>
- [23] D. Kulić, C. Ott, D. Lee, J. Ishikawa, and Y. Nakamura, “Incremental learning of full body motion primitives and their sequencing through human motion observation,” *The Int. Journal of Robotics Research*, vol. 31, no. 3, pp. 330–345, 2012.
- [24] P. Kratzer, M. Toussaint, and J. Mainprice, “Towards combining motion optimization and data driven dynamical models for human motion prediction,” in *IEEE-RAS Int. Conf. on Humanoid Robots (Humanoids)*. IEEE, 2018, pp. 202–208.
- [25] K. Fragkiadaki, S. Levine, P. Felsen, and J. Malik, “Recurrent network models for human dynamics,” in *IEEE Int. Conf. on Computer Vision (ICCV)*, 2015, pp. 4346–4354.
- [26] P. Kratzer, M. Toussaint, and J. Mainprice, “Prediction of human full-body movements with motion optimization and recurrent neural networks,” in *IEEE Int. Conf. Robotics And Automation (ICRA)*, 2020.
- [27] M. Ghallab, D. Nau, and P. Traverso, *Automated Planning: theory and practice*. Elsevier, 2004.
- [28] T. Siméon, J.-P. Laumond, J. Cortés, and A. Sahbani, “Manipulation planning with probabilistic roadmaps,” *The Int. Journal of Robotics Research*, vol. 23, no. 7-8, pp. 729–746, 2004.
- [29] L. P. Kaelbling and T. Lozano-Pérez, “Hierarchical task and motion planning in the now,” in *IEEE Int. Conf. Robotics And Automation (ICRA)*. IEEE, 2011, pp. 1470–1477.
- [30] N. T. Dantam, Z. K. Kingston, S. Chaudhuri, and L. E. Kavraki, “An incremental constraint-based framework for task and motion planning,” *The International Journal of Robotics Research*, vol. 37, no. 10, pp. 1134–1151, 2018.
- [31] T. Lozano-Pérez and L. P. Kaelbling, “A constraint-based method for solving sequential manipulation planning problems,” in *2014 IEEE/RSJ International Conference on Intelligent Robots and Systems*. IEEE, 2014, pp. 3684–3691.
- [32] F. Lagriffoul, D. Dimitrov, J. Bidot, A. Saffiotti, and L. Karlsson, “Efficiently combining task and motion planning using geometric constraints,” *The International Journal of Robotics Research*, vol. 33, no. 14, pp. 1726–1747, 2014.
- [33] M. Toussaint and M. Lopes, “Multi-bound tree search for logic-geometric programming in cooperative manipulation domains,” in *2017 IEEE International Conference on Robotics and Automation (ICRA)*. IEEE, 2017, pp. 4044–4051.
- [34] M. Fox and D. Long, “Pddl2.1: An extension to pddl for expressing temporal planning domains,” *Journal of Artificial Intelligence Research*, vol. 20, p. 61–124, Dec 2003. [Online]. Available: <http://dx.doi.org/10.1613/jair.1129>
- [35] P. Kratzer, N. B. Midlagajni, M. Toussaint, and J. Mainprice, “Anticipating human intention for full-body motion prediction in object grasping and placing tasks,” in *IEEE Int. Symp. on Robot and Human Interactive Communication (RO-MAN)*, 2020.